© 2014. Published by The Company of Biologists Ltd | Development (2014) 141, 1544-1552 doi:10.1242/dev.099986

RESEARCH ARTICLE

Distinct Notch signaling outputs pattern the developing arterial system

Aurelie Quillien[1], John C. Moore[1,‡], Masahiro Shin[1], Arndt F. Siekmann[1,*], Tom Smith[1], Luyuan Pan[2], Cecilia B. Moens[2], Michael J. Parsons[3] and Nathan D. Lawson[1,§]

ABSTRACT

Differentiation of arteries and veins is essential for the development of a functional circulatory system. In vertebrate embryos, genetic manipulation of Notch signaling has demonstrated the importance of this pathway in driving artery endothelial cell differentiation. However, when and where Notch activation occurs to affect endothelial cell fate is less clear. Using transgenic zebrafish bearing a Notch-responsive reporter, we demonstrate that Notch is activated in endothelial progenitors during vasculogenesis prior to blood vessel morphogenesis and is maintained in arterial endothelial cells throughout larval stages. Furthermore, we find that endothelial progenitors in which Notch is activated are committed to a dorsal aorta fate. Interestingly, some arterial endothelial cells subsequently downregulate Notch signaling and then contribute to veins during vascular remodeling. Lineage analysis, together with perturbation of both Notch receptor and ligand function, further suggests several distinct developmental windows in which Notch signaling acts to promote artery commitment and maintenance. Together, these findings demonstrate that Notch acts in distinct contexts to initiate and maintain artery identity during embryogenesis.

KEY WORDS: Notch, Artery differentiation, Vascular system, Zebrafish

INTRODUCTION

Establishment of arterial and venous identity is among the earliest endothelial differentiation steps to occur in the developing vascular system. Although these differences were historically attributed to physiological forces associated with blood flow, more recent studies demonstrated that conserved developmental signaling pathways govern artery and vein identity (Swift and Weinstein, 2009). Furthermore, numerous studies have found that specification of arterial and venous endothelial cell fates is essential for normal vascular morphogenesis and function in vertebrate embryos (Seo et al., 2006; Wang et al., 1998; You et al., 2005). Importantly, the failure to maintain artery identity through conserved developmental signaling pathways may lead to vascular malformations in adults (Carlson et al., 2005; Murphy et al., 2009). Thus, patterning artery and vein identity is essential for normal embryonic development and subsequent circulatory function.

[1]Program in Gene Function and Expression, UMass Medical School, Worcester, MA 01605 USA. [2]Division of Basic Sciences, Fred Hutchinson Cancer Research Center, 1100 Fairview Ave. North, Mail Stop B2-152, Seattle, WA 98109-1024, USA. [3]Institute of Genetic Medicine, Johns Hopkins University, 733 N Broadway, Broadway Research Bldg 469, Baltimore, MD 21205, USA.
*Present address: Max-Planck-Institute for Molecular Biomedicine, Roentgenstr. 20, 48149 Muenster, Germany. ‡Present address: Massachusetts General Hospital, 149 13th Street, Charlestown, MA 02129, USA.

§Author for correspondence (nathan.lawson@umassmed.edu)

Received 10 June 2013; Accepted 28 January 2014

By early-somitogenesis stages of embryonic development, endothelial progenitors, or angioblasts, initiate expression of endothelial cell-specific genes and coalesce to form nascent cords that will give rise to the major blood vessels (Cleaver and Krieg, 2010). Subsequently, expression of artery-specific genes can be detected (Zhong et al., 2001), suggesting that artery and vein specification is an early step during vascular development. Indeed, lineage tracing of progeny from lateral mesoderm progenitors at mid-somitogenesis stages reveals artery or vein lineage commitment by this stage (Kohli et al., 2013; Zhong et al., 2001). Subsequently, artery differentiation appears to be important for vascular morphogenesis. For example, loss of the artery-specific transmembrane ligand, ephrinB2, or its receptor EphB4, which is preferentially expressed in venous endothelial cells, causes similar defects in vascular morphogenesis (Gerety et al., 1999; Wang et al., 1998). Notably, ephrinB2 and EphB4 play important roles in sorting cells at boundary domains within tissues such as the hindbrain (Xu et al., 1999), suggesting that these receptors play a similar role in artery and vein formation. Indeed, ephrinB2 or EphB4 deficiency in zebrafish disrupts segregation of arterial and venous endothelial cell during vessel morphogenesis (Herbert et al., 2009). Thus, differentiation of artery and vein identity governs vascular morphogenesis, in part by establishing the appropriate complement of guidance molecules to distinctly mark and sort these cell populations.

The first genes to be implicated in arterial endothelial specification were components of the Notch signaling pathway (Lawson et al., 2001). Notch proteins are large transmembrane receptors that govern fate decisions in numerous cell types in all animal species studied to date (Guruharsha et al., 2012). Notch receptors are activated by binding to transmembrane molecules known as Delta-like or Jagged ligands. Following binding, the intracellular domain of the processed Notch receptor translocates into the nucleus where it interacts with the Suppressor of hairless/recombination signal binding protein for immunoglobulin kappa J (Rbpj) DNA-binding protein to form a transactivation complex that induces target gene expression (Bailey and Posakony, 1995; Fortini and Artavanis-Tsakonas, 1994). In most cases, the net outcome of this signaling event is that ligand- and receptor-expressing cells will adopt distinct cell fates or exhibit different behaviors in the context of a developing tissue (Guruharsha et al., 2012). During vascular development, Notch receptors and ligands are preferentially expressed in arterial endothelial cells (Lawson et al., 2001; Villa et al., 2001). Accordingly, Notch deficiency leads to a failure in artery marker gene expression, along with the appearance of arteriovenous shunts, in both mouse and zebrafish embryos (Krebs et al., 2004; Lawson et al., 2001). Loss of Notch also leads to a ‘hyper-angiogenesis’ phenotype characterized by increased proliferation and migration of endothelial cells and the excessive formation of non-functional blood vessels (Hellström et

Development (2014) doi:10.1242/dev.099986

al., 2007; Leslie et al., 2007; Siekmann and Lawson, 2007b; Suchting et al., 2007). In these cases, Notch acts to appropriately coordinate tip and stalk cell behaviors in a sprouting blood vessel, in part by dampening the response to surrounding pro-angiogenic factors. In addition to its requirement for vascular development, Notch signaling is also essential for vessel homeostasis in the adult. For example, similar to Delta-like 4 (Dll4) in the embryonic vasculature, Dll1 is restricted to arterial endothelial cells in adult blood vessels, where it is required for collateral artery remodeling (Limbourg et al., 2007). Thus, Notch signaling plays a number of roles within endothelial cells to govern artery differentiation, angiogenesis, and vascular homeostasis during both embryonic and adult stages.

Notch signaling is highly dynamic and can be used reiteratively during the commitment and differentiation of cell lineages (Guruharsha et al., 2012). Although we have learned a great deal concerning the role of Notch in vascular development from genetic manipulations in model systems, we still know little about when and where Notch is activated in endothelial cells during embryogenesis. We previously generated zebrafish lines that allow visualization of Notch-responsive cells and lineage tracing of progeny cells in which Notch has been activated (Clements et al., 2011; Lorent et al., 2010; Parsons et al., 2009; Quillien et al., 2011; Wang et al., 2011). In the study reported here, we have applied these transgenic lines together with genetic manipulation of Notch receptors and ligands, to investigate the dynamic role of Notch signaling during vascular development. Our results suggest that Notch acts at several distinct developmental stages through the use of different receptor and ligand combinations to govern multiple stages of artery formation and patterning.

RESULTS

Notch is activated in arterial endothelial cells and their progenitors

To determine when Notch is activated in endothelial cells during development, we performed two-color fluorescence *in situ* hybridization on embryos with a Notch-responsive promoter (referred to as '*tp1*') driving enhanced green fluorescent protein [*Tg(tp1:egfp)*^{um14} (Parsons et al., 2009)]. At the five somite stage (ss), we observed *egfp* transcript in presumptive somitic mesoderm and proneural clusters (Fig. 1A), as well as neural crest cells located dorsal to cells expressing *ets variant gene 2* (*etv2*) (Fig. 1A,B), an early marker for endothelial progenitors (Sumanas and Lin, 2006). We noted rare *etv2*-positive cells expressing *egfp* at this stage, but not earlier (Fig. 1B,C, yellow arrows; data not shown). By the 12 ss, increasing numbers of *etv2*-positive cells expressed *egfp* and they were intermingled with *egfp*-negative angioblasts (Fig. 1D,E). At the 16 ss, we noted graded levels of *egfp* expression in *fli1a*-positive endothelial cells forming the aortic cord (Fig. 2A,B). At this stage, endothelial cells located more rostrally expressed high levels of *egfp*, whereas caudal cells exhibited lower expression (Fig. 2B, compare cells indicated by yellow arrowheads and white arrows, respectively). *Egfp* expression in *fli1a*-positive cells in the developing aorta continued to increase in a rostral to caudal pattern until 24 hours postfertilization (hpf) when all cells within the dorsal aorta expressed high levels of *egfp* (compare Fig. 2A,C,D). We observed continued expression of Egfp in endothelial cells lining intersomitic arteries and the dorsal aorta in *Tg(fli1a:dsredex)*^{um13}*;(tp1:egfp)*^{um14} double transgenic embryos until at least 7 days postfertilization (Fig. 2E). In addition to endothelial expression, we also noted rare *egfp*-positive *gata1a*-expressing cells in the early lateral mesoderm, whereas *egfp* and *cmyb* expression were largely non-overlapping during mid-somitogenesis stages (supplementary material Fig. S1). *Egfp* expression did not expand in these populations, as we observed with *etv2*- or *fli1a*-positive cells, although *egfp*-positive *cmyb*-expressing cells were apparent in the ventral wall of the dorsal aorta at the 18 ss (supplementary material Fig. S1; data not shown). These observations suggest that Notch activation initiates in *etv2*-positive endothelial progenitors during the earliest stages of vasculogenesis. Subsequently, Notch activation was restricted to and persisted in arterial endothelial cells throughout later embryonic and larval stages.

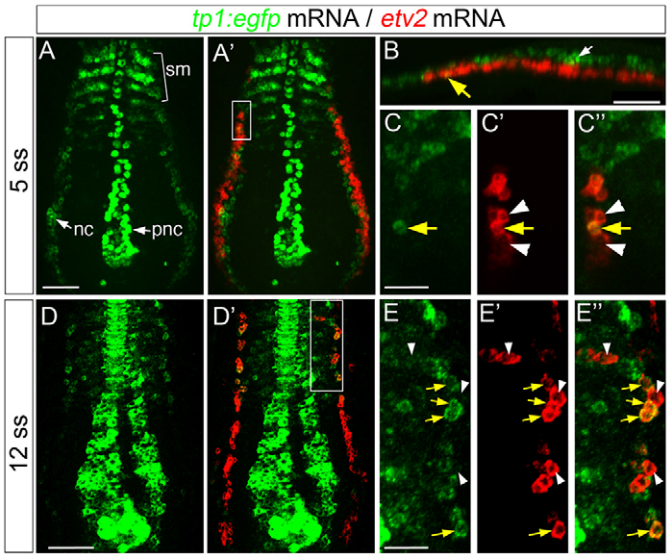

Fig. 1. Notch signaling is active in early endothelial progenitors. (A-E) Confocal micrographs of flat-mounted *Tg(tp1:egfp)*^{um14} embryos following fluorescence *in situ* hybridization using riboprobes against *egfp* (green) and *etv2* (red). (A,C-E) Dorsal views. (A-C) Images from the same embryo at 5 ss. (A,D) *tp1:egfp* expression; (A′,D′) *tp1:egfp* plus *etv2* expression. (A) Arrows indicate neural crest (nc), proneural clusters (pnc); bracket denotes somitic mesoderm (sm). (B) Lateral view of embryo in A showing *egfp* expression in neural crest (white arrow), dorsal to *etv2*-expressing cells. The yellow arrow denotes the *egfp*/*etv2*-positive cell shown in C-C″; white arrowheads indicate the *etv2*-positive/*egfp*-negative cells. (C) Magnified area indicated by box in A′. (D,E) Images of the same embryo at 12 ss. (D′) Box indicates area magnified in E. (E) White arrowheads indicate *etv2*-positive/*egfp*-negative cells; yellow arrows denote *egfp*/*etv2*-coexpression. Scale bars: 100 µm (A,B,D); 40 µm (C,E).

To determine the fate of cells in which Notch activation occurred during early somitogenesis, we performed lineage tracing using *Tg(tp1:creert2)*^{jh12} transgenic zebrafish that express a tamoxifen-inducible form of Cre recombinase driven by the *tp1* element (Wang et al., 2011). For this purpose, we pulsed *Tg(tp1:creert2)*^{jh12} embryos bearing a ubiquitously expressed conditional *hmgb1-mcherry* fusion [*Tg(actb2:loxP-stop-loxP;hmgb1-mcherry)*^{jh15}] with tamoxifen for 1 hour at the 5 or 10 ss. After 48 hours, we observed red fluorescent cells lining the dorsal aorta, but not the cardinal vein in *Tg(tp1:creert2)*^{jh12}*;(actb2:loxP-stop-loxP;hmgb1-mcherry)*^{jh15} embryos (Fig. 3A; *n*=28 embryos). We similarly observed aorta-restricted expression in *Tg(tp1:creert2)*^{jh12} embryos bearing an endothelial-specific conditional red fluorescent transgene [*Tg(fli1ep:loxP-nblue-loxP;mcherry)*^{um43}] at 30 hpf following a 1 hour exposure to tamoxifen at the 10 ss (Fig. 3B; *n*=28 embryos from three separate clutches with contribution to the aorta, but not the vein). Taken together, these results suggest that Notch activation marks endothelial progenitors committed to a dorsal aorta fate.

Development (2014) doi:10.1242/dev.099986

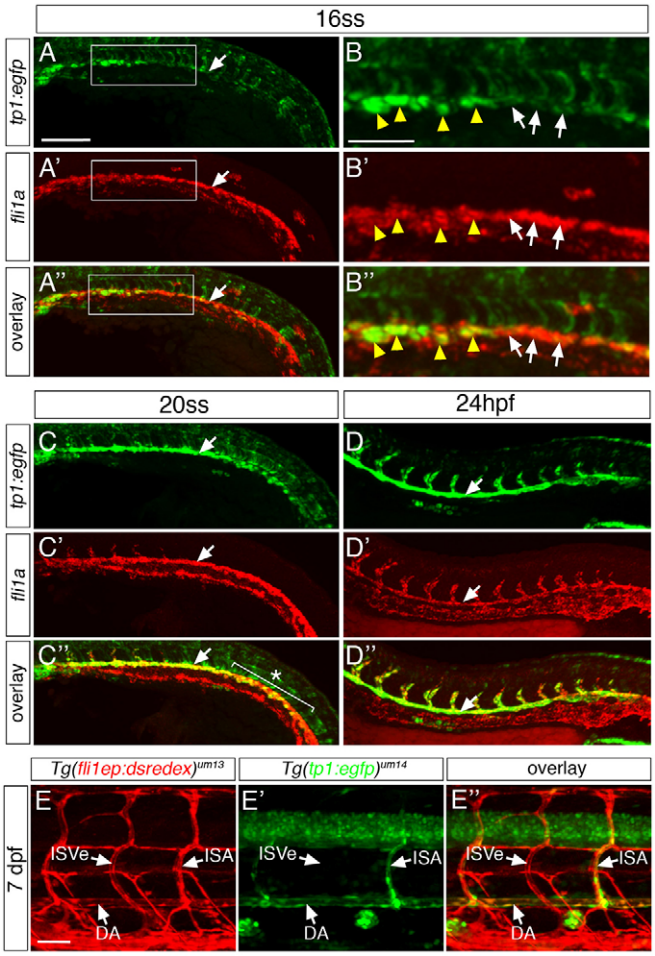

Fig. 2. Notch activity increases and persists in arterial endothelial cells at later developmental stages. (A-D) Confocal micrographs of *Tg(tp1:egfp)*^{um14} embryos following fluorescence *in situ* hybridization using riboprobes against *egfp* (green) and *fli1a* (red). Lateral views, dorsal is up, anterior to the left. (A,C,D) White arrows denote dorsal aorta. (A) 16 ss embryo; the white box indicates the magnified area shown in B. (B) Yellow arrowheads and white arrows denote endothelial cells with high and low *egfp* expression, respectively. (C) Embryo at the 20 ss; the bracket with an asterisk in C″ shows area of mixed high- and low-expressing *egfp*-positive endothelial cells. (D) Embryo at 24 hpf. (E) Confocal micrograph of live *Tg(fli1a:dsredex)*^{um13}*;(tp1:egfp)*^{um14} embryo at 7 days postfertilization showing Notch activation (green) and endothelial cells (red); DA, dorsal aorta; ISA, intersomitic artery; ISVe, intersomitic vein. Scale bars: 100 µm (A,C,D); 50 µm (B,E).

Multiple Notch receptors and ligands contribute to artery differentiation

Within the developing zebrafish vascular system, *notch1a*, *notch1b* and *notch3* are expressed in arterial endothelial cells (Geudens et al., 2010; Lawson et al., 2001; Leslie et al., 2007) (supplementary material Fig. S2A). To determine their contribution to endothelial Notch activation and arterial differentiation, we assessed expression of *tp1:egfp* and endogenous *efnb2a* (ephrin B2a) in embryos lacking different combinations of Notch receptors. Knockdown of *notch1a* or *notch1b* alone had no effect on Notch activation at early stages (supplementary material Fig. S2B; data not shown), whereas *notch3*^{fh332} mutant embryos lost *tp1:egfp* expression in endothelial progenitors compared with wild-type siblings (Fig. 4A,B). Despite this defect, *notch3*^{fh332} mutant embryos exhibited both *tp1:egfp* and *efnb2a* expression at 24 hpf in dorsal aorta endothelial cells, albeit at lower levels compared with wild-type siblings (Fig. 4C,D), suggesting a compensatory role for *notch1a* or *notch1b*. Indeed, *tp1:egfp* and *efnb2a* expression was extinguished in *notch3*^{fh332} mutant embryos injected with a *notch1b* morpholino oligonucleotide (MO), but reduction of *notch1b* alone had no effect (Fig. 4E,F). Knockdown of *notch1a* alone also had no major effect on *tp1:egfp* or *efnb2a* expression (supplementary material Fig. S3A,B), similar to *notch1a*^{tp37} mutant embryos (data not shown), which are adult viable (van Eeden et al., 1996). However, combined loss of *notch1a* and *notch1b*, or *notch1a* and *notch3*, further reduced *tp1:egfp* and *efnb2a* expression (supplementary material Fig. S3C,D).

Loss of general Notch signaling components (e.g. Rbpj) causes circulatory defects, including cranial hemorrhage and arteriovenous shunts between trunk blood vessels, and increased endothelial cell numbers in sprouting intersomitic vessels (ISVs) (Lawson et al., 2001; Leslie et al., 2007; Siekmann and Lawson, 2007b). However, embryos lacking each individual receptor exhibited normal trunk circulation (supplementary material Movies 1-4 and Fig. S4A), whereas only *notch3*^{fh332} mutant embryos exhibited cranial hemorrhage (supplementary material Fig. S4A), as recently reported (Wang et al., 2014; Zaucker et al., 2013). We also noted increased numbers of ISV endothelial cells only in embryos deficient for *notch1b* (supplementary material Fig. S4B). Although loss of single receptors did not affect circulatory patterns, combined loss of different receptor pairs caused qualitatively distinct defects. For example, reduction of *notch1b* in *notch3*^{fh332} mutant embryos increased the penetrance of cranial hemorrhage and caused loss of trunk blood flow (supplementary material Fig. S2C and Fig. S4A). In some of these cases, a poorly formed dorsal aorta and cardinal vein accompanied the circulatory block (supplementary material Movie 5), although active arteriovenous shunts were not generally observed (supplementary material Fig. S4A). We also noted embryos in which aorta and vein morphology appeared normal, but few blood cells were in circulation (supplementary material Movie 6), possibly due to the occurrence of severe cranial hemorrhage. Injection of *notch1b* MO into *notch1a*^{tp37} mutant embryos also caused a block in trunk circulation, although we never observed hemorrhage in these embryos (supplementary material Fig. S4A). Furthermore, arteriovenous shunts between the aorta and vein were apparent in *notch1a*^{tp37}*;notch1b* MO embryos (supplementary material Movie 7 and Fig. S4A). Taken together, these observations suggest multiple Notch receptors together contribute to artery differentiation during vascular development. However, there appear to be distinct roles for receptors in governing different aspects of subsequent vascular morphogenesis and circulatory function.

In mouse embryos, the Notch ligand Dll4 is required for both artery differentiation and angiogenesis (Hellström et al., 2007; Krebs et al., 2004). However, zebrafish embryos deficient for *dll4* display hyperangiogenesis but normal artery differentiation (Leslie et al., 2007; Siekmann and Lawson, 2007b), suggesting a role for other ligands. A possible candidate is Deltac (Dlc), which is similar to both Dll1 and Dll4, and is expressed in posterior somitic mesoderm and in arterial endothelial cells (Smithers et al., 2000). In *Tg(tp1:egfp)*^{um14} embryos, Deltac exhibits punctate localization, indicative of its engagement with Notch receptors (Wright et al., 2011), within somite cells adjacent to Etv2/EGFP-positive cells (Fig. 5A,B). These observations suggest that Deltac may be responsible for Notch activation in endothelial progenitors. Accordingly, *egfp* expression was lost in *etv2*-positive angioblasts of *Tg(tp1:egfp)*^{um14} embryos injected with *deltac* MO, compared with control MO (Fig. 5C,D). Despite this effect, zebrafish mutant for *dlc* survive to adulthood (Jülich et al., 2005) and exhibit normal

Development (2014) doi:10.1242/dev.099986

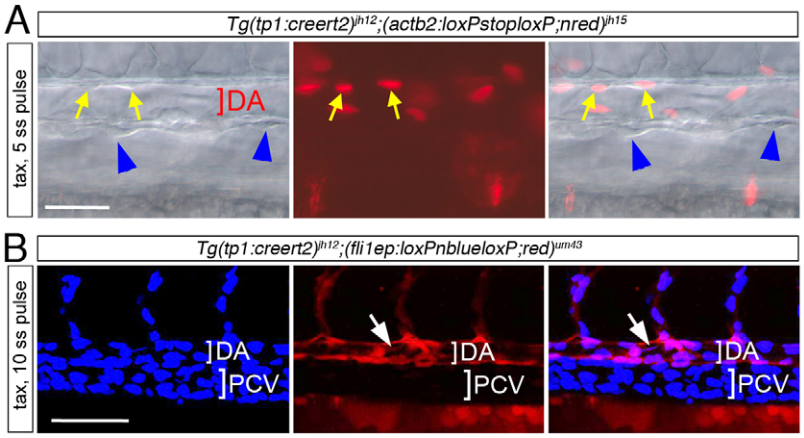

Fig. 3. Cells exhibiting early Notch activation contribute to the dorsal aorta. Lateral views, dorsal is up, anterior to the left. (A) *Tg(tp1:creert2)*^{jh12}*; (actb2:loxP-stop-loxP;nred)*^{jh15} embryo at 48 hpf following exposure to tamoxifen at 5 ss for 1 hour. Left: differential interference contrast (DIC) image; middle: epifluorescence; right: overlay image. Yellow arrows denote presumptive endothelial cells lining the dorsal aorta (red bracket); blue arrowheads label non-fluorescent venous endothelial cells. (B) Two-photon microscopy of a *Tg(tp1:creert2)*^{jh12}*;(fli1ep:loxP-nblue-loxP;red)*^{um43} embryo at 30 hpf following exposure to tamoxifen at 10 ss for 1 hour. Left: blue fluorescence in all endothelial nuclei; middle: red fluorescence in lineage traced endothelial cells; right: overlay. Arrow denotes red fluorescent endothelial cells in the dorsal aorta (DA); PCV, posterior cardinal vein. Scale bars: 50 μm.

artery identity and cardiovascular function (supplementary material Fig S4C and Movie 8; data not shown) as described previously (Shaw et al., 2006). However, reduction of *dll4* in *dlc*^{tit446} mutant embryos, but not wild-type siblings, caused loss of both *efnb2a* and *tp1:egfp* transgene expression in arterial endothelial cells (Fig. 5E,F; data not shown). Likewise, circulation was normal in *dll4*-deficient wild-type embryos, whereas heterozygous and homozygous *dlc*^{tit446} embryos lacking *dll4* showed increasing penetrance of trunk circulatory defects, including arteriovenous shunts (supplementary material Fig. S4C and Movies 9-11). Additionally, combined loss of *dlc* and *dll4* led to low penetrance of cranial hemorrhaging, similar to *notch3*^{fh332} mutant embryos (data not shown).

Dynamic Notch activation during arteriovenous remodeling

ISV endothelial cells sprout from the dorsal aorta and initially exhibit artery identity (Bussmann et al., 2010; Geudens et al., 2010; Isogai et al., 2003; Siekmann and Lawson, 2007b). However, approximately half of the ISVs later regress from the aorta and connect to intersomitic vein (ISVe) sprouts from the posterior cardinal vein to establish a functional circulatory loop (Isogai et al., 2003). During this process, arterial endothelial cells in remodeled ISVes appear to progressively lose arterial identity (Bussmann et al., 2010). Furthermore, *notch1b* and *dll4* are required for maintenance of arterial ISV connections to the dorsal aorta, suggesting a role for Notch in regulating this process (Geudens et al., 2010; Leslie et al., 2007). Because our initial lineage-tracing observations suggested that early Notch activation led to arterial endothelial commitment, we wanted to determine whether early activation might influence the identity of ISV endothelial cells. For this purpose, we pulsed *Tg(tp1:creert2)*^{jh12}*;(actb2:loxP-stop-loxP;nred)*^{jh15} embryos with tamoxifen at different stages and observed the distribution of labeled cells in intersomitic arteries (ISA) or ISVe at 60 hpf. Interestingly, cells labeled at the 5-10 ss were equally distributed between ISA or ISVe (Fig. 6A,B), despite their initial restriction to the dorsal aorta (see Fig. 3). Thus, early Notch activation can bestow positional determination but does not irrevocably commit cells to an arterial fate. A similar distribution in ISV contribution was apparent until 36-48 hpf, when there was a clear shift toward a contribution to only intersomitic arteries (Fig. 6B; data not shown).

Our results suggest that ISV endothelial cells derive from an early Notch-positive angioblast and that persistence or downregulation of Notch activity in these cells determines identity as an artery or a vein, respectively. To further investigate this possibility, we utilized *Tg(tp1:kaede)*^{um15} embryos in which the *tp1* element drives expression of the photoconvertible Kaede fluorescent protein (Clements et al., 2011). Following exposure of *Tg(tp1:kaede)*^{um15} embryos to UV light at 36 hpf, we observed photoconverted red fluorescence in ISVs at 60 hpf (Fig. 6C), consistent with initial Notch activation in these cells at 36 hpf. Furthermore, ISVs showing green fluorescence, indicative of persistent Notch signaling following photoconversion, retained their connection to the dorsal aorta (Fig. 6C,D, white arrows), whereas those displaying only red fluorescence were connected to the posterior cardinal vein (Fig. 6C,D, yellow arrows). These results suggest that ISV endothelial cells derive from angioblasts in which Notch was activated but subsequent reduction in Notch activity in some cells caused them to lose artery identity and become incorporated into veins. Given the importance of *notch1b* and *dll4* in the control of ISV identity (Geudens et al., 2010; Leslie et al., 2007), we reasoned that they maintain Notch activation at later developmental stages in endothelial cells lining the ISVs. Accordingly, loss of either *notch1b* or *dll4* completely eliminated *tp1:egfp* expression in ISV endothelial cells, at 30 hpf (Fig. 6E-G), whereas loss of *notch3* had no effect (Fig. 6H). We also observed decreased *egfp* levels within the neural tube of *notch1b*-deficient embryos (Fig. 6F). Interestingly, *tp1:egfp* levels in the dorsal aorta were also decreased at 30 hpf following loss of *notch1b* or *dll4*, although they were individually dispensable for *egfp* expression at earlier stages (compare Fig. 6F,G; Fig. 4E, left panel; data not shown). Consistent with our observations and previously published studies (Geudens et al., 2010), most ISVs in *dll4*- or *notch1b*-deficient embryos retain venous connections, whereas arterial connections are normal in *dlc*^{tit446}, *notch1a*^{tp37} and *notch3*^{fh332} mutant embryos (supplementary material Fig. S5). These observations suggest that *dll4* and *notch1b* are specifically required for maintaining Notch activation and arterial identity in endothelial cells at later stages of vascular development.

DISCUSSION

Our observations using zebrafish bearing *tp1*-driven transgenes, together with genetic manipulation of Notch receptors and ligands, suggest a series of Notch-dependent decisions that pattern the arterial system in the zebrafish embryo (Fig. 7). We first observe Notch activation in *etv2*-positive endothelial progenitors at the 5 ss and lineage tracing demonstrates that these cells, or their progeny, are committed to contribute to the dorsal aorta. These results are consistent with previous lineage analyses in zebrafish, which demonstrated that cells within the lateral mesoderm are restricted to artery or vein fate as early as the 7 ss (Kohli et al., 2013; Zhong et al., 2001). We postulate that cells committed to the aorta in those studies probably exhibited Notch activation. At this early stage, endothelial Notch activation appears to be induced by Deltac-positive somitic mesoderm. However, this signaling event does not

Development (2014) doi:10.1242/dev.099986

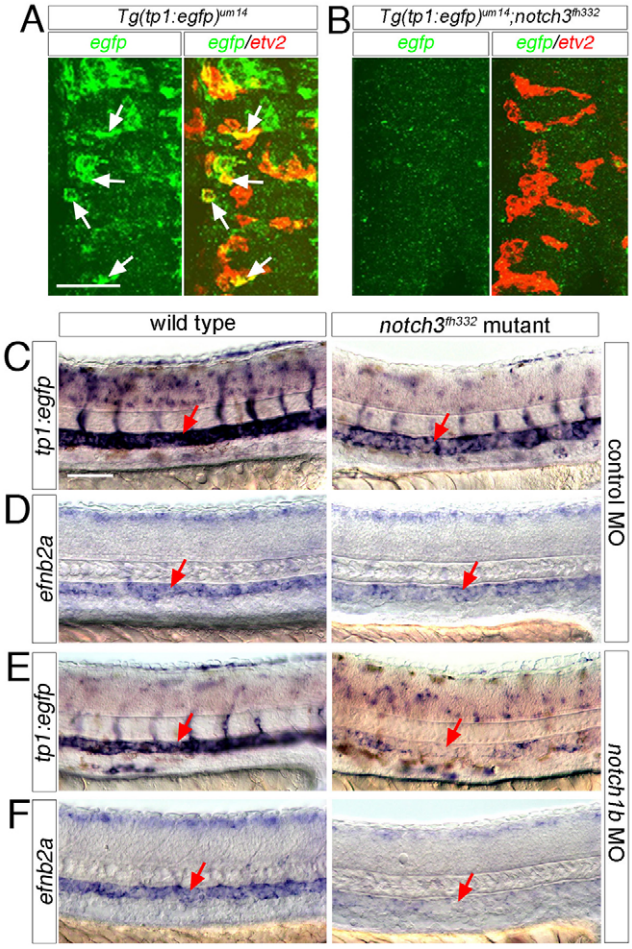

Fig. 4. Multiple Notch receptors contribute to artery differentiation. (A,B) Confocal micrographs of flat-mounted sibling embryos at 10 ss following fluorescence *in situ* hybridization with riboprobes against *egfp* (green) and *etv2* (red). Dorsal view, anterior is up. (A) Wild type *Tg(tp1:egfp)*^{um14}; arrows indicate *etv2*/*egfp* double-positive cells. (B) *Tg(tp1:egfp)*^{um14}*;notch3*^{fh332} mutant sibling. (C-F) DIC images of *Tg(tp1:egfp)*^{um14} wild-type (left panels) and *notch3*^{fh332} mutant (right panels) embryos at 24 hpf subjected to *in situ* hybridization with riboprobes against *egfp* (C,E) or *efnb2a* (D,F); (C,D) Embryos injected with 2.5 ng control morpholino (MO). (E,F) Embryos injected with 2.5 ng *notch1b* MO. Scale bars: 40 µm (A,B); 50 µm (C-F).

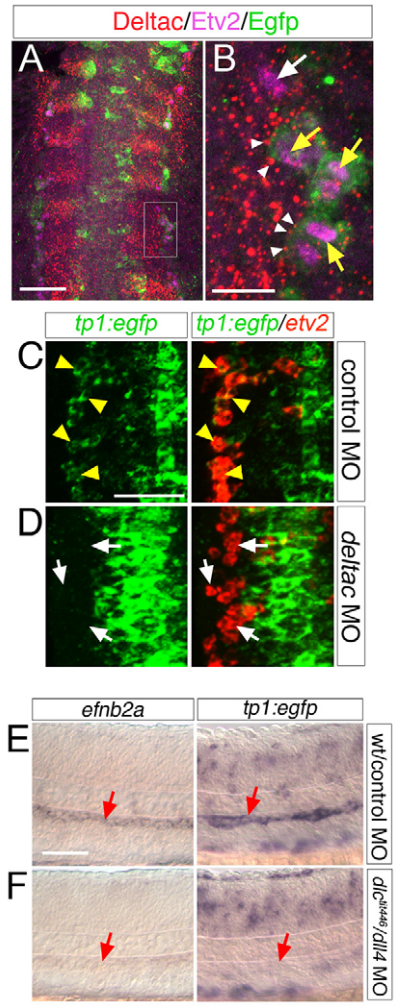

Fig. 5. *deltac* and *dll4* have overlapping roles during artery differentiation. (A) Flat-mounted *Tg(tp1:egfp)*^{um14} embryo at 12 ss immunostained with antibodies against Deltac (red), Etv2 (magenta) and Egfp (green). Dorsal view, anterior is up. Box indicates magnified region in B. (B) White arrow denotes nucleus of Egfp-negative, Etv2-positive endothelial progenitor. Yellow arrows denote Etv2-positive nuclei of Egfp-positive cells. White arrowheads mark Deltac puncta adjacent to Egfp-positive endothelial cells. (C,D) Flat-mounted *Tg(tp1:egfp)*^{um14} embryos at 10 ss following two-color fluorescence *in situ* hybridization with riboprobes against *egfp* (green) and *etv2* (red) imaged by confocal microscopy. Dorsal view, anterior is up. Yellow arrowheads denote *etv2*/*egfp*-positive cells; white arrows are *etv2*/*egfp*-negative cells. Embryos injected with 10 ng of control MO (C), or 10 ng of *deltac* MO (D). (E,F) DIC images of *Tg(tp1:egfp)*^{um14} embryos subjected to whole-mount *in situ* hybridization with riboprobes against *efnb2a* (left panels) or *egfp* (right panels). (E) Wild-type embryo injected with 15 ng control MO. (F) *dlc*^{tit446} mutant embryo injected with 15 ng *dll4* MO. Scale bars: 40 µm (A,C); 10 µm (B); 50 µm (E,F).

irrevocably determine identity because progeny can later be found in intersomitic veins. Surprisingly, *notch3* and *dlc*, which are both required for early Notch activation in *etv2*-positive cells, alone are dispensable for arterial differentiation. Rather, early Notch activation might simply provide a positional cue to separate presumptive dorsal aorta and cardinal vein cell populations. Even in the absence of this signal, a general migration of all mesodermal types, including endothelial progenitors, to the midline occurs during somitogenesis. At this point, stochastic sorting could allow sufficient numbers of endothelial cells to be in position to receive a Notch-dependent, pro-artery differentiation signal in the absence of an initial directed guidance cue. This might provide an explanation of why early Notch activation by *notch3* and *dlc* is dispensable for later artery differentiation.

Temporal analysis of *tp1:egfp* expression suggests that a second wave of Notch activation occurs after cells reach the midline and begin to form the dorsal aorta. Our results suggest that at least three different Notch receptors (*notch1a*, *notch1b* and *notch3*), together with two separate ligands (*dll4* and *dlc*) contribute to overall activation in this developmental window and that this activation contributes, in part, to artery differentiation. This is consistent with our previous work demonstrating that endothelial cell-autonomous Notch activation in this window induces artery differentiation and preferential dorsal aorta localization (Lawson et al., 2002; Siekmann and Lawson, 2007b). Whether the requirement for multiple receptors reflects simultaneous signaling to a required activation threshold, or is reflective of qualitatively distinct outputs is not clear. The partial reduction in arterial *tp1:egfp* and *efnb2a* expression at

Development (2014) doi:10.1242/dev.099986

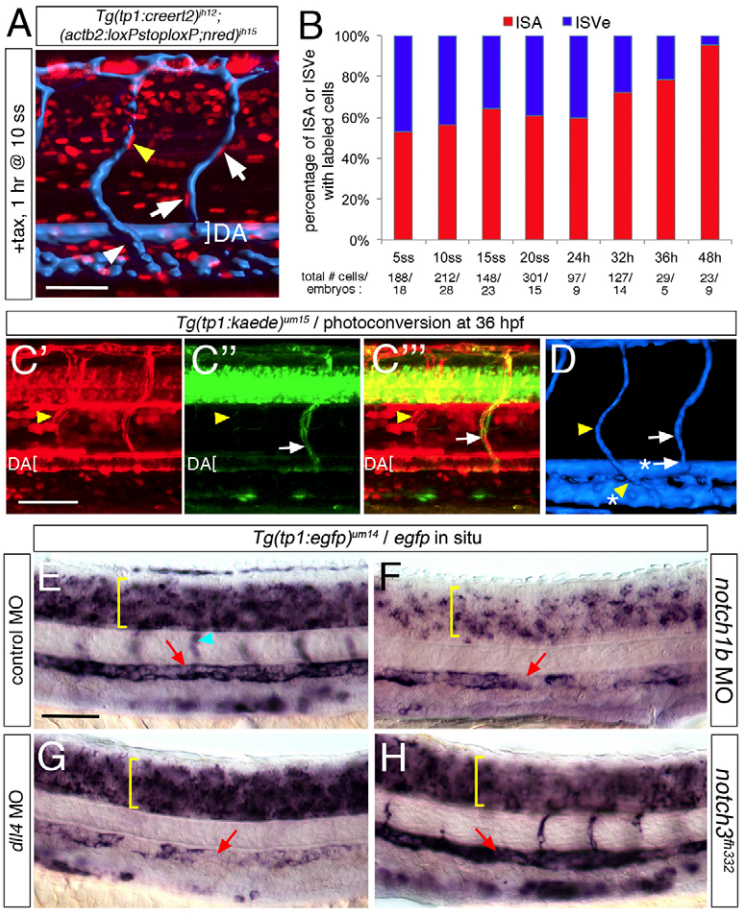

Fig. 6. Notch is downregulated in ISVs during arteriovenous reprogramming. (A) Two-photon imaging following microangiography (surface-rendered in blue) of *Tg(tp1:creert2)*^{jh12}*;(actb2:loxP-stop-loxP;nred)*^{jh15} embryo at 60 hpf following exposure to tamoxifen at 10 ss for 1 hour. Yellow arrowhead denotes red endothelial nucleus lining an intersomitic vein, as determined by its connection to the posterior cardinal vein (white arrowhead). White arrows indicate cells lining an intersomitic artery connected to the dorsal aorta (indicated by white bracket). (B) Graph showing proportion of intersomitic arteries or veins with red fluorescent cells in *Tg(tp1:creert2)*^{jh12}*;(fli1ep:loxPnBlueloxP;red)*^{um43} embryos at 60 hpf following a 1 hour tamoxifen pulse at the indicated stage; total numbers of labeled cells and embryos counted are indicated below the *x*-axis. (C,D) Two-photon micrographs of same *Tg(tp1:kaede)*^{um15} embryo at 60 hpf following photoconversion of Kaede at 36 hpf. Yellow arrowheads denote intersomitic vein endothelial cell positive for red, but not green fluorescence. White arrow denotes an intersomitic artery endothelial cell that maintained Kaede expression. (C) Red fluorescence indicating cells that exhibited Notch activation upon photoconversion at 36 hpf. (C′) Green fluorescence from Kaede expressed after photoconversion. (C″) Overlay of images in C and C′. (D) Surface rendering of image stack following microangiography of embryo in C; asterisked arrowhead and arrow denote connection to posterior cardinal vein and dorsal aorta, respectively. (E-H) *Tg(tp1:egfp)*^{um14} embryos at 30 hpf subjected to whole-mount *in situ* hybridization with an *egfp* riboprobe. Embryos injected with 2.5 ng of control MO (E), 2.5 ng of *notch1b* MO (F), 15 ng of *dll4* MO (G) or mutant for *notch3*^{fh332} (H). Yellow bracket denotes neural tube, light blue arrowhead indicates the intersomitic vessels, and red arrow indicates the dorsal aorta. Scale bars: 50 µm.

24 hpf following loss of single Notch receptors, along with complete loss accompanying deficiency in different receptor combinations might suggest the former. However, differences in circulatory defects associated with distinct receptor knockdowns, as well as unique phenotypes associated with single receptor deficiencies clearly suggest there are qualitative differences between receptor outputs (Fig. 7). In any case, a better understanding of the downstream regulatory cascades that are affected by each receptor may begin to provide some insight into how they work together to contribute to artery differentiation and vascular morphogenesis.

Although multiple notch receptors appear to contribute to arterial differentiation in the aorta, there are also subsequent stage- and cell-type-specific requirements for *notch1b*. Together with *dll4*, *notch1b* is essential for maintaining Notch activation in arterial endothelial cells in both the dorsal aorta and developing ISAs at later stages. Previous studies have shown that hyperangiogenesis defects are apparent in embryos deficient only for *notch1b* or *dll4* (Leslie et al., 2007; Siekmann and Lawson, 2007b), suggesting a specific role of this ligand–receptor pair in controlling angiogenic cell behaviors. Taken with previous observations, our current work suggests that *dll4* and *notch1b* promote the decision of an arterial endothelial cell to remain as such rather than becoming a tip cell and sprouting out of the dorsal aorta (Fig. 7, ~24-30 hours). We envisage that this process is probably governed by lateral inhibition, in which Notch acts to define distinct fates in two adjacent equipotent cells. This is consistent with previous models in which high levels of Vegfa, experienced by cells in the dorsal aorta near the somite boundary, induces expression of the Notch ligand Dll4 (Siekmann and Lawson, 2007a). This would in turn activate Notch1b in the adjacent cell to prevent migration out of the dorsal aorta and reinforce an arterial endothelial cell fate. Thus, the second wave of *tp1:egfp* induction observed as cells reach the midline might be, in part, a consequence of Notch activation in the selection of patent arterial endothelial cells versus sprouting tip cells (Fig. 7). It is likely that this process is then reiteratively used following cell division of the tip cell in the sprouting ISV. Whether this decision point is linked to the later fate of the ISV as arterial or venous is unknown. Based on the pattern of *tp1:egfp* reporter expression and lineage tracing of Notch-activated cells during sprouting, we would propose that these are distinct processes.

An interesting finding from our lineage-tracing studies is that cells in which Notch was activated at early stages can later contribute to ISVes. Despite the initial positional commitment of these Notch-activated cells to the dorsal aorta, our observations suggest that arterial endothelial cells can later de- or trans-differentiate to become venous tissue. These findings are consistent with those in chick embryos, which found that arterial endothelial cells transplanted into a vein would adopt venous identity, although this plasticity was limited to the earliest stages of development (Moyon et al., 2001). Accordingly, veins grafted into coronary arteries in rats exhibit de-differentiation of venous identity, but fail to acquire artery marker gene expression, suggesting limited plasticity in adult vessels (Kudo et al., 2007). Despite this finding, ectopic activation of Notch in adult vasculature is capable of modulating artery identity, leading to arteriovenous malformations (Carlson et al., 2005), suggesting that mature endothelial cells retain the ability to re-program their identity under some settings. Our results suggest that venous reprogramming is associated with downregulation of Notch activity, consistent with

Development (2014) doi:10.1242/dev.099986

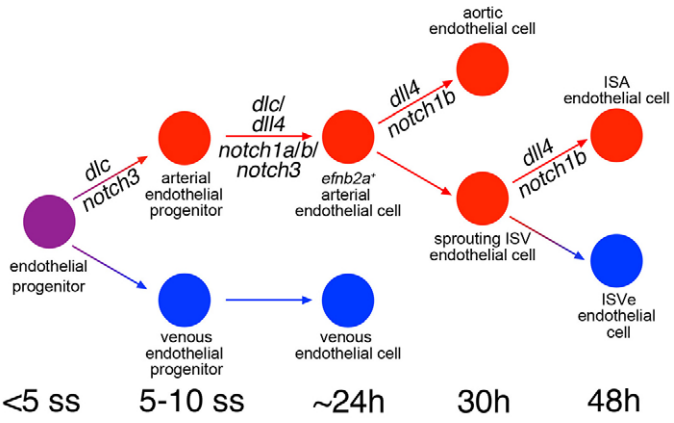

Fig. 7. Model of the dynamic roles of Notch signaling during artery development.

previous work in which *notch1b* or *dll4* deficiency causes the formation of excessive venous ISV connections (Geudens et al., 2010). Interestingly, venous ISVs in which Notch signaling is downregulated do not appear to gain a hyper-angiogenic phenotype, as is observed when Notch signaling is lost in all ISVs [e.g. *dll4* deficiency (Leslie et al., 2007; Siekmann and Lawson, 2007b)]. This might reflect an early requirement for Notch in limiting angiogenesis only during initial ISV sprouting when there is probably an increase in pro-angiogenic signaling, compared with later stages when ISV remodeling occurs. Thus, it is likely that *notch1b* and *dll4*, which are required to both limit angiogenesis and maintain ISV artery identity, are acting in distinct contexts during each of these processes (Fig. 7).

A number of approaches have been applied to determine the spatial and temporal control of Notch activation during development. These include transgenic mice bearing a Notch-responsive element comprising three Rbpj-binding sites (Duncan et al., 2005) or the *tp1* element driving *lacZ* (Souilhol et al., 2006). Both lines have been helpful to visualize Notch activation in the embryonic and postnatal vascular system. Although *tp1*-driven Cre lines have not been developed, Vooijs et al. generated mice in which the intracellular domain of the Notch1 receptor was fused in frame with Cre recombinase (NIPCre) to allow lineage tracing of progeny, and these cells exhibit Notch1 activation (Vooijs et al., 2007). However, NIPCre-labeled cells are permanently marked by the initial Notch signal, making it difficult to assess dynamic changes. These mouse models also suffer from the difficulty in making serial temporal observations during development. In this regard, our application of the *tp1* element in zebrafish embryos, which are transparent and develop externally, provides a major benefit. Using a combination of *tp1*-driven transgenes and genetic manipulation of Notch signaling components, we were able to ascertain when and where particular Notch ligands and receptors are required for activation. In parallel, our use of a *tp1*:CreERT line allowed us to follow progeny cells after Notch activation. In this case, the ability to limit tamoxifen treatment to a narrow developmental stage allowed precise definition of when Notch signaling is affecting lineage decisions. Despite the benefits of the *tp1* promoter, a drawback is that it reports signaling mediated through Rbpj, which is commonly used by all Notch receptors for target gene expression (Guruharsha et al., 2012), making it challenging to discern receptor-specific signaling events. Although combining genetic manipulation of Notch signaling with the *tp1*-driven transgenes has been helpful, generation of receptor-specific sensors, similar to NIP-Cre, or Gal4 fusions used successfully in *Drosophila* (Struhl and Adachi, 1998), will be needed moving forward.

MATERIALS AND METHODS

Zebrafish care and maintenance

Zebrafish (*Danio rerio*) and their embryos were handled according to standard protocols and in accordance with accepted University of Massachusetts Medical School IACUC protocols. The establishment and characterization of *Tg(fli1ep:dsredex)*^{um13}, *Tg(tp1:egfp)*^{um14}, *Tg(tp1:creert2)*^{jh12}, *Tg(tp1:kaede)*^{um43}, *Tg(actb2:loxP-stop-loxP;hmgb1-mcherry)*^{jh15} [referred to hereafter as *Tg(actb2:loxP-stop-loxP;nred)*^{jh15}], *notch1a*^{tp37}, *deltac*^{tit446}, *dll4*^{j16e1} and *notch3*^{fh332} have been described elsewhere (Clements et al., 2011; Covassin et al., 2009; Holley et al., 2002; Jülich et al., 2005; Leslie et al., 2007; Parsons et al., 2009; Zaucker et al., 2013). Lines generated in this study are described below.

Plasmid construction

To construct a conditional endothelial marker transgene, we cloned the *fli1ep* fragment (Villefranc et al., 2007) into pDestTol2pA (Kwan et al., 2007) using PspOMI after removing ATGs between the PspOMI site and attR4 site to give pTol-*fli1ep*R4-R3pA. In parallel, a monomeric form of mCerulean fused to H2B was cloned between direct *loxP* repeats flanked by attL4 and attR1 to give p5E-loxP-*nBlue-loxP*. We performed a multisite LR reaction using p5E-lox*P-nBlue-loxP*, pME-mCherry and an empty p3E-mcs-1 vector with pTol-*fli1ep*R4-R3pA to give pTol-*fli1ep:loxP-nBlue-loxP;mcherry*.

Microinjections

deltac, *dll4* and *notch1a* morpholino oligonucleotides (MOs) are described elsewhere (Holley et al., 2002; Siekmann and Lawson, 2007b). The sequence of the splice blocking Notch1b MO, which targets the exon 8 splice donor site, is 5′-GTTCCtCCgGTTACCTGGCATACAG-3′; lowercase letters denote two mismatches compared with Zv9 reference sequence. MOs were dissolved in nuclease-free water (Ambion). Embryos from incrosses of indicated heterozygous carriers or wild-type adults were injected at the one- to two-cell stage with 15 ng *dll4*, 2.5 ng *notch1b* MO, or 1 ng *notch1a* MO, respectively, or comparable amount of scrambled (control) MO. We confirmed the effect of the *notch1b* on splicing by RT-PCR of *notch1b* from RNA isolated from MO-injected embryos using the following primers: forward, 5′-GTTGGGCCGGCCTGTGAC-3′; reverse, 5′-CTCGCACA-GACGGCCC-3′. The *Tg(fli1ep:loxP-nblue-loxP;red)*^{um43} line was generated using pTol-*fli1ep:loxP-nBlue-loxP;mcherry* by Tol2 transposition as described previously (Covassin et al., 2009).

In situ hybridization

Whole-mount *in situ* hybridization was performed using standard protocols (Hauptmann and Gerster, 2000). *efnb2a* riboprobe preparation has been described elsewhere (Lawson et al., 2001). The antisense *egfp* riboprobe was prepared by linearizing pENTR-EGFP2 (Villefranc et al., 2007) with *Nco*I followed by *in vitro* transcription using T7 polymerase. Stained embryos were imaged by differential interference contrast (DIC) microscopy using an Axiophot2 (Zeiss) and a W Plan-Apochromat 20×/1.0 (NA) DIC D=0.17 M27 75 mm, and images were captured using an AxioCam hRC (Zeiss). For fluorescence *in situ* hybridization, *etv2* and *egfp* templates were generated by PCR with a custom SP6 (5′-gcttgatttaggtgacactat-3′) and a standard M13 reverse primer from pCS2-*etv2* (Moore et al., 2013) and pCS2-*egfp* (Villefranc et al., 2007) templates, respectively. Antisense *etv2* or *egfp* riboprobes were synthesized from these templates using T3 RNA polymerase and DIG-dUTP or fluorescein-dUTP, respectively. Hybridization and detection was carried out using the TSA Plus system (PerkinElmer) as follows: *Tg(tp1:egfp)*^{um14} embryos at 10-12 ss were fixed with 4% paraformaldehyde in 1× phosphate-buffered saline (PFA/PBS) overnight at 4°C, transferred to methanol, and washed with 3% H_2O_2/methanol for 1 hour. Embryos were washed with methanol and stored at –20°C until use. Standard hybridization and washing was performed (Hauptmann and Gerster, 2000) and embryos were placed in maleic acid buffer (MAB; 150 mM maleic acid/100 mM NaCl (pH 7.5)/2% blocking reagent; Roche). Embryos were incubated overnight at 4°C in MAB containing 1:1000 sheep anti-DIG antibody conjugated to horseradish

peroxidase (POD; Roche). Embryos were washed with MAB/0.001% Tween 20 six times at room temperature, once with PBS, and placed in 1:50 tyramide-Cy3/1× amplification diluent buffer for 3 hours to detect *etv2* mRNA. Embryos were washed with PBS/0.1% Tween 20 (PBST) overnight at room temperature and placed in methanol. To quench POD activity, stained embryos were treated with 3% H_2O_2/methanol for 30 minutes at room temperature and washed with PBST, followed by MAB/0.001% Tween 20. *Egfp* mRNA was detected as above, except that 1:500 POD-conjugated anti-fluorescein (Roche) and 1:50 tyramide-FITC were used. Double-stained embryos were briefly washed with PBST, flat mounted, and imaged with a Leica confocal TCS SP2 microscope using an oil immersion 40× HC x PL APO CS (NA=1.25). Vertical projections were assembled using Imaris or the Fiji package of ImageJ.

Immunostaining

Tg(tp1:egfp)^{um14} embryos were fixed in 4% PFA/PBS for 15 minutes at room temperature, washed with methanol, quenched with 3% H_2O_2 in methanol for 1 hour at room temperature and stored in methanol at −20°C before use. Embryos were washed with TBST (Tris-buffered saline/0.1% Tween 20) plus 0.1% Triton X-100 and permeabilized with TBST/0.5% Triton X-100 for 30 minutes at room temperature. After blocking with TBST containing 1% BSA and 10% goat serum, embryos were incubated with 1:250 mouse anti-DeltaC antibody (zdc2; Abcam) and 1:500 rabbit anti-zebrafish Etv2 (Moore et al., 2013) in blocking buffer overnight at 4°C. Embryos were washed briefly and incubated with 2% blocking reagent/MAB, followed by HRP-conjugated goat anti-mouse IgG (H+L) at 1:1000 and goat anti-rabbit IgG (H+L) conjugated to Alexa Fluor 633 (Invitrogen, cat. no. A-21070) at 1:500 overnight at 4°C. The embryos were washed with MAB, followed by 1× PBS and incubated with tyramide-Cy3 diluted 1:50 in 1× amplification diluent (PerkinElmer) for 3 hours at room temperature. Subsequently, HRP activity was quenched with 3% H_2O_2/methanol for 1 hour at room temperature. Embryos were washed in TBST, followed by incubation with 2% blocking reagent/MAB and then 1:1000 goat anti-GFP–HRP (Rockland). After washing with MAB and 1× PBS, embryos were incubated with 1:50 tyramide-FITC in 1× amplification diluent (PerkinElmer). Embryos were flat mounted and imaged using confocal microscopy as above.

Cre/lox lineage tracing

Embryos from crosses between *Tg(tp1:creert2)^{jh12}* and either *Tg(actb2:loxP-stop-loxP;nred)^{jh15}* or *Tg(fli1ep:loxP-nblue-loxP;nred)^{um43}* carriers were placed in standard egg water containing 0.5 µM 4-hydroxy-tamoxifen (Sigma) diluted from a 10 mM stock in ethanol for 1 hour at the indicated developmental stages. Embryos were washed successively with 800 ml and 50 ml egg water and grown to the indicated stage. Tamoxifen-treated *Tg(tp1:creert2)^{jh12};(actb2:loxP-stop-loxP;nred)^{jh15}* embryos were imaged at 30 hpf by DIC and epifluorescence microscopy using an Axioplan2 and a water immersion 20× lens (NA=1) or subjected to microangiography using blue fluorescent 0.02 µm carboxylate-modified Fluospheres (Life Technologies) and imaged with a LSM 7MP laser scanning microscope (Zeiss) equipped with a Chameleon Ti:Sapphire pulsed laser (Coherent) using ZEN 2009 software (Zeiss). Red, green and blue fluorescence was sequentially excited at 1034, 890 and 760 nm, respectively. Emissions were captured using separate detectors with 565-610 (red), 500-550 (green) and 400-480 nm (blue) band pass filters. Labeled progeny cells in *Tg(tp1:creert2)^{jh12};(fli1ep:loxP-nblue-loxP;red)^{um43}* embryos were similarly imaged by two-photon microscopy using sequential excitation at 1034 and 890 nm. Blue fluorescence was detected using a band pass filter at 440-475 nm and mCherry was detected as above. For assessment of contribution to arterial or venous ISVs, *Tg(tp1:creert2)^{jh12};(fli1ep:loxP-nblue-loxP;red)^{um43}* embryos were observed at 60 hpf after tamoxifen treatment as described in the text. ISVs in which labeled cells were found were defined as arterial or venous based on the direction of circulatory flow as determined by light microscopy.

Kaede photoconversion

Tg(tp1:kaede)^{um43} embryos were mounted on depression slides in 5% methylcellulose at 36 hpf and illuminated for 20 seconds with UV-wavelength light on an Axiophot2 (Zeiss) microscope using a 20× lens (NA=1). Both red and green emissions were immediately checked following UV exposure to confirm complete photoconversion. Embryos were returned to egg water at 28°C until 60 hpf. Red and green fluorescence were detected on a Leica confocal TCS SP2 microscope or embryos were subjected to microangiography and two-photon imaging as above.

Assessment of circulatory function and genotyping

Embryos deficient for different combinations of Notch receptor or ligand function were observed, using a dissection microscope at 72 hpf, for circulation through the trunk blood vessels and presence of cranial hemorrhage. Following phenotypic assessment, embryos were subjected to genotyping using primers flanking mutations in *dlc* (forward, 5′-GAAA-CAAACATTGACGACTGCTCAAGCGACCCC-3′; reverse, 5′-GTCCTT-GCCTGAGAAACC-3′) or *notch3* (forward, 5′-CCCTGAAGGGTTCC-ATGATCCCTACTACTA-3′; reverse, 5′-TCCAGGCTCACAGTCACACC-GATA-3′). Amplicons were digested with either *Psh*AI (*dlc*) or *Spe*I (*notch3*) and separated by gel electrophoresis. Circulatory defects were captured by video micrography on a Zeis Axophot2 microscope equipped with a DMK 21AU04 digital video camera (Imaging Source). Movies were labeled and compressed using Flash (Adobe) and Quicktime (Apple) software, respectively.

Acknowledgements

We would like to thank present and past members of the Lawson laboratory for helpful insights in the course of this work. We thank George Kourkoulis and Ira Male for technical assistance. We also thank John Polli and Ed Jaskolski for fish care and maintenance.

Competing interests

The authors declare no competing financial interests.

Author contributions

A.Q., J.C.M., M.S., A.F.S., T.S. and N.D.L. designed and performed experiments and analyzed data. N.D.L. wrote the paper. L.P. and C.B.M. identified the *notch3^{fh332}* line and M.J.P. generated the *Tg(tp1:creert2)^{jh12}* and *Tg(actb2:loxP-stop-loxP;nred)^{jh15}* lines.

Funding

This was work was supported by the National Heart, Lung and Blood Institute [R01HL093467 to N.D.L.; R01HD076585 to C.B.M.; R01DK080730 to M.J.P.] and a pre-doctoral fellowship from the American Heart Association [0815732D to J.C.M.]. Deposited in PMC for release after 12 months.

Supplementary material

Supplementary material available online at
http://dev.biologists.org/lookup/suppl/doi:10.1242/dev.099986/-/DC1

References

Bailey, A. M. and Posakony, J. W. (1995). Suppressor of hairless directly activates transcription of enhancer of split complex genes in response to Notch receptor activity. *Genes Dev.* **9**, 2609-2622.

Bussmann, J., Bos, F. L., Urasaki, A., Kawakami, K., Duckers, H. J. and Schulte-Merker, S. (2010). Arteries provide essential guidance cues for lymphatic endothelial cells in the zebrafish trunk. *Development* **137**, 2653-2657.

Carlson, T. R., Yan, Y., Wu, X., Lam, M. T., Tang, G. L., Beverly, L. J., Messina, L. M., Capobianco, A. J., Werb, Z. and Wang, R. (2005). Endothelial expression of constitutively active Notch4 elicits reversible arteriovenous malformations in adult mice. *Proc. Natl. Acad. Sci. USA* **102**, 9884-9889.

Cleaver, O. and Krieg, P. A. (2010) Vascular development. In *Heart Development and Regeneration* (ed. N. Rosenthal and R. P. Harvey), pp. 487-528. London, UK: Academic Press.

Clements, W. K., Kim, A. D., Ong, K. G., Moore, J. C., Lawson, N. D. and Traver, D. (2011). A somitic Wnt16/Notch pathway specifies haematopoietic stem cells. *Nature* **474**, 220-224.

Covassin, L. D., Siekmann, A. F., Kacergis, M. C., Laver, E., Moore, J. C., Villefranc, J. A., Weinstein, B. M. and Lawson, N. D. (2009). A genetic screen for vascular mutants in zebrafish reveals dynamic roles for Vegf/Plcg1 signaling during artery development. *Dev. Biol.* **329**, 212-226.

Duncan, A. W., Rattis, F. M., DiMascio, L. N., Congdon, K. L., Pazianos, G., Zhao, C., Yoon, K., Cook, J. M., Willert, K., Gaiano, N. et al. (2005). Integration of Notch and Wnt signaling in hematopoietic stem cell maintenance. *Nat. Immunol.* **6**, 314-322.

Fortini, M. E. and Artavanis-Tsakonas, S. (1994). The suppressor of hairless protein participates in notch receptor signaling. *Cell* **79**, 273-282.

Gerety, S. S., Wang, H. U., Chen, Z. F. and Anderson, D. J. (1999). Symmetrical mutant phenotypes of the receptor EphB4 and its specific transmembrane ligand ephrin-B2 in cardiovascular development. *Mol. Cell* **4**, 403-414.
Geudens, I., Herpers, R., Hermans, K., Segura, I., Ruiz de Almodovar, C., Bussmann, J., De Smet, F., Vandevelde, W., Hogan, B. M., Siekmann, A. et al. (2010). Role of delta-like-4/Notch in the formation and wiring of the lymphatic network in zebrafish. *Arterioscler. Thromb. Vasc. Biol.* **30**, 1695-1702.
Guruharsha, K. G., Kankel, M. W. and Artavanis-Tsakonas, S. (2012). The Notch signalling system: recent insights into the complexity of a conserved pathway. *Nat. Rev. Genet.* **13**, 654-666.
Hauptmann, G. and Gerster, T. (2000). Multicolor whole-mount in situ hybridization. *Methods Mol. Biol.* **137**, 139-148.
Hellström, M., Phng, L. K., Hofmann, J. J., Wallgard, E., Coultas, L., Lindblom, P., Alva, J., Nilsson, A. K., Karlsson, L., Gaiano, N. et al. (2007). Dll4 signalling through Notch1 regulates formation of tip cells during angiogenesis. *Nature* **445**, 776-780.
Herbert, S. P., Huisken, J., Kim, T. N., Feldman, M. E., Houseman, B. T., Wang, R. A., Shokat, K. M. and Stainier, D. Y. (2009). Arterial-venous segregation by selective cell sprouting: an alternative mode of blood vessel formation. *Science* **326**, 294-298.
Holley, S. A., Jülich, D., Rauch, G. J., Geisler, R. and Nüsslein-Volhard, C. (2002). her1 and the notch pathway function within the oscillator mechanism that regulates zebrafish somitogenesis. *Development* **129**, 1175-1183.
Isogai, S., Lawson, N. D., Torrealday, S., Horiguchi, M. and Weinstein, B. M. (2003). Angiogenic network formation in the developing vertebrate trunk. *Development* **130**, 5281-5290.
Jülich, D., Hwee Lim, C., Round, J., Nicolaije, C., Schroeder, J., Davies, A., Geisler, R., Lewis, J., Jiang, Y. J., Holley, S. A.; Tübingen 2000 Screen Consortium (2005). beamter/deltaC and the role of Notch ligands in the zebrafish somite segmentation, hindbrain neurogenesis and hypochord differentiation. *Dev. Biol.* **286**, 391-404.
Kohli, V., Schumacher, J. A., Desai, S. P., Rehn, K. and Sumanas, S. (2013). Arterial and venous progenitors of the major axial vessels originate at distinct locations. *Dev. Cell* **25**, 196-206.
Krebs, L. T., Shutter, J. R., Tanigaki, K., Honjo, T., Stark, K. L. and Gridley, T. (2004). Haploinsufficient lethality and formation of arteriovenous malformations in Notch pathway mutants. *Genes Dev.* **18**, 2469-2473.
Kudo, F. A., Muto, A., Maloney, S. P., Pimiento, J. M., Bergaya, S., Fitzgerald, T. N., Westvik, T. S., Frattini, J. C., Breuer, C. K., Cha, C. H. et al. (2007). Venous identity is lost but arterial identity is not gained during vein graft adaptation. *Arterioscler. Thromb. Vasc. Biol.* **27**, 1562-1571.
Kwan, K. M., Fujimoto, E., Grabher, C., Mangum, B. D., Hardy, M. E., Campbell, D. S., Parant, J. M., Yost, H. J., Kanki, J. P. and Chien, C. B. (2007). The Tol2kit: a multisite gateway-based construction kit for Tol2 transposon transgenesis constructs. *Dev. Dyn.* **236**, 3088-3099.
Lawson, N. D., Scheer, N., Pham, V. N., Kim, C. H., Chitnis, A. B., Campos-Ortega, J. A. and Weinstein, B. M. (2001). Notch signaling is required for arterial-venous differentiation during embryonic vascular development. *Development* **128**, 3675-3683.
Lawson, N. D., Vogel, A. M. and Weinstein, B. M. (2002). sonic hedgehog and vascular endothelial growth factor act upstream of the Notch pathway during arterial endothelial differentiation. *Dev. Cell* **3**, 127-136.
Leslie, J. D., Ariza-McNaughton, L., Bermange, A. L., McAdow, R., Johnson, S. L. and Lewis, J. (2007). Endothelial signalling by the Notch ligand Delta-like 4 restricts angiogenesis. *Development* **134**, 839-844.
Limbourg, A., Ploom, M., Elligsen, D., Sörensen, I., Ziegelhoeffer, T., Gossler, A., Drexler, H. and Limbourg, F. P. (2007). Notch ligand Delta-like 1 is essential for postnatal arteriogenesis. *Circ. Res.* **100**, 363-371.
Lorent, K., Moore, J. C., Siekmann, A. F., Lawson, N. and Pack, M. (2010) Reiterative use of the notch signal during zebrafish intrahepatic biliary development. *Dev. Dyn.* **239**, 855-864.
Moore, J. C., Sheppard-Tindell, S., Shestopalov, I. A., Yamazoe, S., Chen, J. K. and Lawson, N. D. (2013). Post-transcriptional mechanisms contribute to Etv2 repression during vascular development. *Dev. Biol.* **384**, 128-140.
Moyon, D., Pardanaud, L., Yuan, L., Bréant, C. and Eichmann, A. (2001). Plasticity of endothelial cells during arterial-venous differentiation in the avian embryo. *Development* **128**, 3359-3370.
Murphy, P. A., Lu, G., Shiah, S., Bollen, A. W. and Wang, R. A. (2009). Endothelial Notch signaling is upregulated in human brain arteriovenous malformations and a mouse model of the disease. *Lab. Invest.* **89**, 971-982.
Parsons, M. J., Pisharath, H., Yusuff, S., Moore, J. C., Siekmann, A. F., Lawson, N. and Leach, S. D. (2009). Notch-responsive cells initiate the secondary transition in larval zebrafish pancreas. *Mech. Dev.* **126**, 898-912.
Quillien, A., Blanco-Sanchez, B., Halluin, C., Moore, J. C., Lawson, N. D., Blader, P. and Cau, E. (2011). BMP signaling orchestrates photoreceptor specification in the zebrafish pineal gland in collaboration with Notch. *Development* **138**, 2293-2302.
Seo, S., Fujita, H., Nakano, A., Kang, M., Duarte, A. and Kume, T. (2006). The forkhead transcription factors, Foxc1 and Foxc2, are required for arterial specification and lymphatic sprouting during vascular development. *Dev. Biol.* **294**, 458-470.
Shaw, K. M., Castranova, D. A., Pham, V. N., Kamei, M., Kidd, K. R., Lo, B. D., Torres-Vasquez, J., Ruby, A. and Weinstein, B. M. (2006). fused-somites-like mutants exhibit defects in trunk vessel patterning. *Dev. Dyn.* **235**, 1753-1760.
Siekmann, A. F. and Lawson, N. D. (2007a). Notch signalling and the regulation of angiogenesis. *Cell Adh. Migr.* **1**, 104-106.
Siekmann, A. F. and Lawson, N. D. (2007b). Notch signalling limits angiogenic cell behaviour in developing zebrafish arteries. *Nature* **445**, 781-784.
Smithers, L., Haddon, C., Jiang, Y. J. and Lewis, J. (2000). Sequence and embryonic expression of deltaC in the zebrafish. *Mech. Dev.* **90**, 119-123.
Souilhol, C., Cormier, S., Monet, M., Vandormael-Pournin, S., Joutel, A., Babinet, C. and Cohen-Tannoudji, M. (2006). Nas transgenic mouse line allows visualization of Notch pathway activity in vivo. *Genesis* **44**, 277-286.
Struhl, G. and Adachi, A. (1998). Nuclear access and action of notch in vivo. *Cell* **93**, 649-660.
Suchting, S., Freitas, C., le Noble, F., Benedito, R., Bréant, C., Duarte, A. and Eichmann, A. (2007). The Notch ligand Delta-like 4 negatively regulates endothelial tip cell formation and vessel branching. *Proc. Natl. Acad. Sci. USA* **104**, 3225-3230.
Sumanas, S. and Lin, S. (2006). Ets1-related protein is a key regulator of vasculogenesis in zebrafish. *PLoS Biol.* **4**, e10.
Swift, M. R. and Weinstein, B. M. (2009). Arterial-venous specification during development. *Circ. Res.* **104**, 576-588.
van Eeden, F. J., Granato, M., Schach, U., Brand, M., Furutani-Seiki, M., Haffter, P., Hammerschmidt, M., Heisenberg, C. P., Jiang, Y. J., Kane, D. A. et al. (1996). Mutations affecting somite formation and patterning in the zebrafish, Danio rerio. *Development* **123**, 153-164.
Villa, N., Walker, L., Lindsell, C. E., Gasson, J., Iruela-Arispe, M. L. and Weinmaster, G. (2001). Vascular expression of Notch pathway receptors and ligands is restricted to arterial vessels. *Mech. Dev.* **108**, 161-164.
Villefranc, J. A., Amigo, J. and Lawson, N. D. (2007). Gateway compatible vectors for analysis of gene function in the zebrafish. *Dev. Dyn.* **236**, 3077-3087.
Vooijs, M., Ong, C. T., Hadland, B., Huppert, S., Liu, Z., Korving, J., van den Born, M., Stappenbeck, T., Wu, Y., Clevers, H. et al. (2007). Mapping the consequence of Notch1 proteolysis in vivo with NIP-CRE. *Development* **134**, 535-544.
Wang, H. U., Chen, Z. F. and Anderson, D. J. (1998). Molecular distinction and angiogenic interaction between embryonic arteries and veins revealed by ephrin-B2 and its receptor Eph-B4. *Cell* **93**, 741-753.
Wang, Y., Rovira, M., Yusuff, S. and Parsons, M. J. (2011). Genetic inducible fate mapping in larval zebrafish reveals origins of adult insulin-producing β-cells. *Development* **138**, 609-617.
Wang, Y., Pan, L., Moens, C. B. and Appel, B. (2014). Notch3 establishes brain vascular integrity by regulating pericyte number. *Development* **141**, 307-317.
Wright, G. J., Giudicelli, F., Soza-Ried, C., Hanisch, A., Ariza-McNaughton, L. and Lewis, J. (2011). DeltaC and DeltaD interact as Notch ligands in the zebrafish segmentation clock. *Development* **138**, 2947-2956.
Xu, Q., Mellitzer, G., Robinson, V. and Wilkinson, D. G. (1999). In vivo cell sorting in complementary segmental domains mediated by Eph receptors and ephrins. *Nature* **399**, 267-271.
You, L. R., Lin, F. J., Lee, C. T., DeMayo, F. J., Tsai, M. J. and Tsai, S. Y. (2005). Suppression of Notch signalling by the COUP-TFII transcription factor regulates vein identity. *Nature* **435**, 98-104.
Zaucker, A., Mercurio, S., Sternheim, N., Talbot, W. S. and Marlow, F. L. (2013). notch3 is essential for oligodendrocyte development and vascular integrity in zebrafish. *Dis. Model. Mech.* **6**, 1246-1259.
Zhong, T. P., Childs, S., Leu, J. P. and Fishman, M. C. (2001). Gridlock signalling pathway fashions the first embryonic artery. *Nature* **414**, 216-220.